

# Photodissociation Dynamics of the Iodine–Arene Charge-Transfer Complex

Egbert Lenderink,<sup>†</sup> Koos Duppen,<sup>†</sup> Frank P. X. Everdij,<sup>†</sup> Janez Mavri,<sup>‡</sup> Renato Torre,<sup>§</sup> and Douwe A. Wiersma<sup>\*,†</sup>

Ultrafast Laser and Spectroscopy Laboratory, Department of Chemical Physics, Materials Science Centre, University of Groningen, Nijenborgh 4, 9747 AG Groningen, The Netherlands, BIOSON Research Institute, Department of Biophysical Chemistry, University of Groningen, Nijenborgh 4, 9747 AG Groningen, The Netherlands, and European Laboratory for Nonlinear Spectroscopy (LENS), University of Florence, Largo E. Fermi 2, 50125 Florence, Italy

Received: November 10, 1995; In Final Form: February 12, 1996<sup>⊗</sup>

The photodissociation reaction of the molecular iodine:arene charge-transfer (CT) complex into an iodine atom and an iodine atom–arene fragment has been investigated using femtosecond pump–probe, resonance Raman, and molecular dynamics simulations. In the condensed phase the reaction proceeds on a time scale of less than 25 fs, in sharp contrast to the gas phase where the excited state lifetime of the complex is about 1 ps. Since little CT resonance enhancement is found in Raman studies on the I<sub>2</sub>-stretch vibration, it is concluded that rapid curve crossing occurs from the CT state to a dissociative surface. Of particular interest is the finding that the polarization anisotropy of the iodine atom:arene (I:ar) photoproduct decays on a time scale of 350 fs both in pure arene solvents as well as in mixed arene/cyclohexane solutions. This latter finding rules out that secondary I:ar complex formation is the main cause of this ultrafast depolarization effect. The initial polarization anisotropy is found to be ~0.12 in pure mesitylene and ~0.34 in mixed mesitylene/cyclohexane solutions. Semiempirical configuration-interaction calculations show that, except for the axial CT complex, the transition dipole is aligned almost parallel to the normal of the arene plane. The oscillator strength of the CT transition is found to be maximal in the oblique conformation with the I<sub>2</sub> molecule positioned at an angle of about 30° with respect to the arene normal. This iodine angular dependence of the oscillator strength leads to photoselection of bent I<sub>2</sub>:ar complexes in pump–probe experiments. Molecular dynamics simulations confirm earlier findings that the I<sub>2</sub>:benzene complex is a fragile entity and that it persists only for a few hundred femtoseconds. These simulations also provide the proper time scale for the decay of the polarization anisotropy. The fact that the photoproduct experiences a substantial torque in the dissociation process explains the absence of a cage effect in this reaction.

## 1. Introduction

One of the main challenges in the field of femtosecond reaction dynamics is the understanding of how ultrafast chemical reactions are affected by their environment.<sup>1</sup> In the past decades seminal experiments were performed on reactions in solutions and in small clusters aimed at, for instance, understanding of the “cage effect”<sup>2</sup> and of the cooling process<sup>3</sup> of reaction products. Often an inert gas solvent was taken<sup>4</sup> to minimize effects caused by solvent–molecule vibrations or by intermolecular interactions. Another advantage of studying reactions in a noble gas environment is that the solute–noble gas potential is well-known,<sup>4</sup> in contrast to the interaction potential between a solute and more common solvents. In biological systems the reaction medium is a protein. Study of protein dynamics is important as it can provide insight into the microscopic proceedings of a biochemical reaction.

A better grasp of solvent and protein dynamics is particularly relevant for electron-transfer reactions. Electron transfer is crucial to the process of photosynthesis,<sup>5</sup> DNA repair,<sup>6</sup> and photovoltaic solar cells.<sup>7</sup> In these reactions the sunlight drives an ultrafast charge-separation reaction at the donor site after which the liberated electron is transferred, often in a sequence of steps, to an acceptor, where the free energy is utilized in a chemical reaction. In simpler donor–acceptor systems, for

instance, intramolecular or bimolecular charge-transfer (CT) complexes, the excited CT state is often short-lived.<sup>8</sup>

In certain charge-transfer complexes the electronic charge distribution in the ground state is only weakly perturbed. Yet, on optical excitation electron transfer determines the reaction path. An example of this type of charge-transfer complex presents the iodine molecule:arene (I<sub>2</sub>:ar) system. In this celebrated charge-transfer complex, a new absorption appears in the near-ultraviolet that is not present in either the donor (arene) or the acceptor (iodine). On optical excitation of the CT band of the I<sub>2</sub>:ar complex, a photochemical reaction occurs. The ensuing photochemistry is particularly simple; it involves the breaking of the iodine–iodine bond and the formation of two radical fragments: an iodine atom and an iodine:arene (I:ar) complex.

About 50 years ago, Benesi and Hildebrand<sup>9</sup> were the first to report on the ultraviolet absorption of the I<sub>2</sub>:benzene complex, and since then the understanding of its spectroscopy and photophysics has been a continuing challenge. The newly formed absorption band in the near-UV was explained by Mulliken<sup>10,11</sup> in terms of a CT excitation, whereby an electron is transferred from the donor D (an arene) to the acceptor A (I<sub>2</sub>):



Although all this was established nearly half a century ago, the exact nature of the CT complex between I<sub>2</sub> and arene is by no means clear. The first Raman studies of I<sub>2</sub> in various arenes<sup>12</sup> seemed to indicate that the complex is not well defined, and it

<sup>†</sup> Ultrafast Laser and Spectroscopy Laboratory, University of Groningen.

<sup>‡</sup> BIOSON Research Institute, University of Groningen.

<sup>§</sup> University of Florence.

<sup>⊗</sup> Abstract published in *Advance ACS Abstracts*, April 1, 1996.

was therefore postulated that  $I_2$  can have weak CT interactions with one or more arene molecules at the same time. A later Raman study by Besnard *et al.*,<sup>13</sup> performed over a broader temperature range, showed that two separate  $I_2$  species exist in liquid benzene, assigned to “free”  $I_2$  and  $I_2$  bound to benzene. The reason that this exchange effect went unnoticed in the earlier study<sup>12</sup> is that the two iodine species interchange very rapidly at room temperature; a lower-limit lifetime of 0.7 ps was obtained.<sup>13</sup>

Meanwhile, the complex was also studied in argon matrices<sup>14</sup> at 77 K. From the infrared and Raman absorption spectra, it was concluded that the point group of the  $I_2$ :benzene ( $I_2$ :ben) complex is  $C_{6v}$ . This means that at least at low temperatures the complex has a well-defined structure, with the  $I_2$  molecular axis coinciding with the 6-fold symmetry axis of benzene; this structure is denoted as “axial”.

Computational studies on the  $I_2$ :ben complex indicate that the complex is rather weakly bound. An early *ab initio* study<sup>15</sup> predicted a low binding energy,  $678\text{ cm}^{-1}$ , which amounts roughly to  $3kT$  at room temperature, thus favoring the view of a bound, but short-lived, complex. However, a semiempirical molecular orbital calculation<sup>16</sup> gave a much higher value for the binding energy:  $6400\text{ cm}^{-1}$ . Both studies<sup>15,16</sup> agreed that the axial conformation is more stable than the “resting” structure, where the  $I_2$  molecule lies parallel to the benzene ring.

The binding energy of the complex in a molecular beam<sup>17</sup> was measured to be  $770\text{ cm}^{-1}$ . Since the *ab initio* calculated binding energy<sup>15</sup> agrees well with experiment, Danten *et al.*<sup>18</sup> used these results in a molecular dynamics calculation of  $I_2$  in liquid benzene. With this parametrization, however, no well-defined  $I_2$ :ben species, either axial or resting, were identified in the simulations. One must conclude that there is always a broad distribution of molecular configurations in solution. This situation then corresponds to the so-called CT-contact limit, where the donor and acceptor of the CT pair are close to each other without being tightly bound. CT-contact pairs have been identified with certainty in the system iodine atom:alkane.<sup>19</sup>

In the past the photochemistry of  $I_2$  in complex-forming solvents has been studied with microsecond,<sup>20</sup> picosecond,<sup>21–23</sup> and femtosecond<sup>24</sup> resolution. Pump–probe measurements on  $I_2$  in arene revealed microsecond-lived transients,<sup>20</sup> which can be assigned to CT complexes of iodine atoms and arene molecules.<sup>23</sup> Picosecond pump–probe studies<sup>21,22</sup> showed that for each dissociation event of an  $I_2$  molecule, two I:ar complexes are formed within the time resolution of the experiments. No other dynamics, such as geminate recombination, could be observed. In pump–probe experiments on the CT band, a second dynamical process was also found. This picosecond-lived transient was attributed by Hilinsky and Rentzepis to the charge separated  $I_2^-:ar^+$  complex.<sup>22</sup> Its decay was attributed to charge recombination.

Recently, we published a Letter on femtosecond pump–probe studies of  $I_2$  in liquid mesitylene and toluene.<sup>24</sup> One of the remarkable observations was that immediately after excitation, the absorption transient was shown to have the spectral content of the I:ar complex, which is one of the photoproducts. For excitation into the CT band, the photodissociation of  $I_2$  in the  $I_2$ :mesitylene ( $I_2$ :mes) and  $I_2$ :toluene ( $I_2$ :tol) complexes thus proceeds within 25 fs. The ultrafast decay of the polarization anisotropy and its low initial value also puzzled us. To explain these observations, we assumed that the CT complex in its transition state is strongly bent along the I–I–mesitylene axis. When an iodine molecule dissociates in this state, one of the iodine atoms moves toward the benzene ring, thereby forcing a rotation of the I:mes product. A second photochemical channel

was also investigated.<sup>25,26</sup> We argued that the corresponding transient is not due to excited-state relaxation of the complex<sup>22</sup> but to dissociation of the complex into arene and molecular  $I_2$ .<sup>24</sup>

Walker *et al.* recently reported<sup>27</sup> femtosecond transient absorption studies on the complex of molecular iodine with hexamethylbenzene in various solvents. They found the initial value of the polarization anisotropy also to be low and very much dependent on the solvent. They interpreted this variation in terms of different equilibrium structures of the complex. However, they also pointed out that the direction of the transition dipole in the CT complex depends very much on the structure of the complex. Thus, without independent knowledge of this structure–transition dipole relation one cannot deduce the structure of the CT complex from the initial value of the polarization anisotropy.

Very recently, Cheng *et al.*<sup>28</sup> performed a femtosecond mass spectrometric study of the photodissociation of  $I_2$ :mes in a molecular beam. In this experiment the iodine atoms, resulting from dissociation of the  $I_2$ :ar complex, were detected by a technique known as “2+1 REMPI.” An iodine atom rise time of about 1 ps was found for the complex (750 fs for  $I_2$ :ben), which indicates that the excited state is formed on a bound potential and that the complex lives for a couple of vibrational periods before it breaks up into products. The relatively slow reaction rate in a beam was explained in terms of a harpoon type mechanism, in which charge reorganization occurs in the transition state before the reaction takes place. The remarkable difference between the solution and gas phase reaction times (25 and 1000 fs ( $I_2$ :mes), respectively) will be addressed in the light of the new results presented here.

In this paper, a more extensive report of femtosecond transient absorption measurements will be presented. Results of a resonance Raman study on the  $I_2$ :mes complex will be presented also. Molecular dynamics studies on the structure and dynamics of the CT complex were also done and will be discussed. A semiempirical configuration-interaction (CI) calculation was carried out to obtain information on the strength and the direction of the transition dipole moment in the  $I_2$ :ben complex. *Ab initio* and molecular dynamics (MD) calculations were used to study the lifetime and stability of the ground-state complex in liquid benzene. The photodissociation of  $I_2$  in the CT complex was also modeled by MD simulations, in an attempt to gain a better understanding of the decay of the polarization anisotropy. These simulations prove our conjecture of a severely bent transition state (to explain the anisotropy data) to be wrong. Yet the calculations suggest a model for the reaction in which photoselection occurs of oblique ground-state conformations, which have a structure very similar to the bent transition state originally proposed. Photoselection of these specific conformations occurs through the strong dependence of the transition dipole on the orientation of the  $I_2$  molecule with respect to the arene. Since predominantly bent  $I_2$ :ar structures are excited, the I:ben photoproduct experiences a torque in the dissociation process, which leads to rapid decay of the polarization anisotropy and prevents recombination due to the cage effect.

The outline of this paper is as follows. Details of the experimental setup are given in section 2, while the results of both femtosecond and Raman experiments are discussed in section 3. In section 4 results of calculations are presented on the relation between the transition dipole moment and the structure of the  $I_2$ :ben complex. Section 5 contains results of molecular dynamics simulations on the stability of the complex in the ground state and on the dynamics of the photodissociation. Finally, in section 6, the results of the experimental and computational results are compared.

## 2. Experimental Section

The femtosecond pump–probe experiments were performed with an amplified CPM dye laser system, described previously.<sup>29</sup> Pump pulses at 310 nm were obtained by second-harmonic generation in KDP. Probe pulses at 620 nm were taken directly from the amplifier. Probe pulses in other parts of the visible spectral region were made by continuum generation. Cross correlations of pump and probe pulses were typically 120–140 fs wide. The sample consisted of a free flowing jet, obtained by pumping the sample solution through a 500  $\mu\text{m}$  sapphire nozzle. More details on the pump–probe experiments can be found in a previous publication.<sup>24</sup>

The resonance Raman experiments were performed with a picosecond dye laser, synchronously pumped by a frequency-doubled mode-locked Nd:YAG laser (Coherent Antares). Its output was amplified in a two-stage dye amplifier (Spectra-Physics), pumped by a frequency-doubled Nd:YAG regenerative amplifier operated at 1 kHz. Various laser and amplifier dye combinations were used to cover the wavelength range from 580 to 710 nm. The picosecond pulses of about 10  $\mu\text{J}$  were frequency doubled in a 7 mm BBO crystal. The sample consisted of a magnetically stirred quartz cell. Care was taken that the excited region was as close to the stirring magnet as possible, to avoid heating or sample degradation effects. The sample solution (o.d.  $\sim 3$ ) was refreshed after every few spectra, and it was checked that the sample's history or lifetime did not affect the results. To minimize reabsorption of Raman scattering, all experiments were performed in a backscattering geometry. The depolarized Raman scattered light was spectrally filtered and dispersed through a triple monochromator system (Jobin-Yvon S3000) and detected by a photodiode array equipped with image intensifier (Princeton). Each data point represents an integrated intensity and was obtained by averaging the Raman signal over 5 min. The error bars represent the maximum signal variation during this time. All data were scaled to the 1000  $\text{cm}^{-1}$  mode of mesitylene, which itself was found not to be resonance enhanced.

Samples were prepared by dissolving iodine (Merck, resublimed) in pure mesitylene (Merck, p.a.) or in mixtures of mesitylene and alkane, the mesitylene concentration being 20% by volume. The studied alkanes were *n*-hexane (Merck, p.a.), cyclohexane (Merck, p.a.), and *n*-hexadecane (Janssen). The concentration of  $\text{I}_2$  in all cases was about  $5 \times 10^{-3}$  M. In pure mesitylene the percentage of  $\text{I}_2$  molecules exhibiting CT absorption was estimated to be 85%.<sup>9</sup> For the mixed solvent samples, this percentage is reduced to 60%, as established by monitoring the intensity of the CT absorption band. When toluene (Merck, p.a.) was used instead of mesitylene, the estimated percentages of "CT-active"  $\text{I}_2$  molecules were 70% for pure toluene solvent and 45% for the toluene/alkane mixtures.

## 3. Results

**3.1. Femtosecond Pump–Probe Experiments.** The pump–probe transient of  $\text{I}_2$  in pure mesitylene, obtained by exciting in the CT band at 310 nm and probing at 620 nm,<sup>24</sup> is displayed in Figure 1. This probe wavelength falls near the maximum of the expected I:mes photoproduct.<sup>23</sup> Measurements at other wavelengths indicate that the spectrum of the instantaneous signal corresponds to the spectrum of the I:mes complex.<sup>20,22</sup> The photoproduct signal is found to rise instantaneously, as can be established by comparing it to the expected signal rise for instantaneous response (shown as a heavy line in Figure 1). The time resolution of the experiment poses an upper limit of 25 fs to the dissociation time of the I–I bond. Apparently,

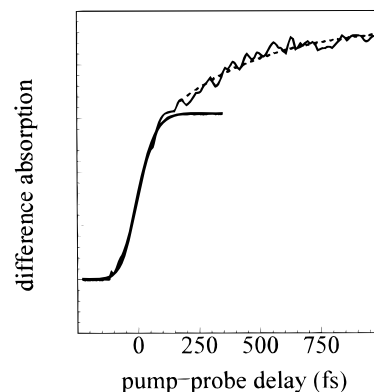


**Figure 1.** Short-time behavior of the pump–probe signal of  $\text{I}_2$  in pure mesitylene. The pump wavelength is 310 nm, the probe wavelength is 620 nm, and the probe is polarized parallel to the pump pulse. The system response function, obtained by integration of the pump–probe cross correlation, is given by the heavy line. The dashed line is a fit of a rising exponential to the data, with a time constant of 400 fs.

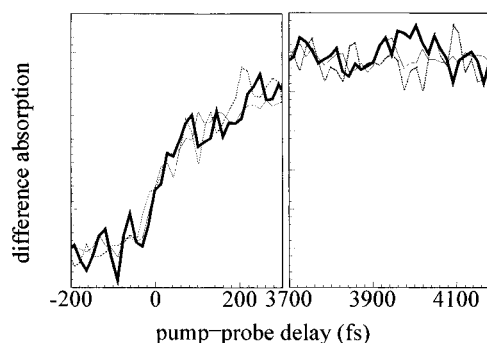


**Figure 2.** Comparison of the signals measured for  $\text{I}_2$ :mes probing at 600 (heavy line), 650 (light line), and 700 nm (dotted line) around  $t = 0$  and around  $t = 4$  ps. The transients were scaled to each other to facilitate comparison; clearly, the short-time spectrum is identical to the one measured at longer time delays.

dissociation occurs on a purely repulsive excited-state potential. The width of the absorption band and its lack of structure would even allow for a dissociation time as short as 2 fs.

Next to the instantaneous component, a signal with a subpicosecond rise time is detected. The dotted line in Figure 1 presents a fit to the signal. A time constant of 400 fs is found.<sup>24</sup> As shown in Figure 2, this 400 fs signal is not accompanied by any spectral change. This precludes an interpretation where the instantaneous signal is attributed to excited-state absorption, and the 400 fs built-up time would reflect the breaking of the I–I bond. Instead, the 400 fs signal is assigned to the formation of a second "batch" of I:mes complexes. These are formed by I atoms launched into the solvent by the dissociation process and which subsequently react with other mesitylene molecules. Strong support for this interpretation is provided by the fact that in mixed mesitylene/alkane solutions no rise in absorption on a 400 fs time scale is observed. This accords with the notion that in mixed mesitylene/alkane solutions there are few free mesitylene molecules available to which react. Figure 3 displays this result. The formation of "secondary" I:mes complexes from its separate constituents thus is a fast process. It may even be barrierless, in which case the time constant is completely determined by diffusion.

The  $\text{I}_2$  dissociation time in arene solutions is thus found to be much faster than that in arene clusters, where 1 ps was obtained for the  $\text{I}_2$ :mes complex.<sup>28</sup> It should be noted that a substantial slowing of photochemical processes in clusters has been observed for other photochemical systems as well.<sup>30</sup>

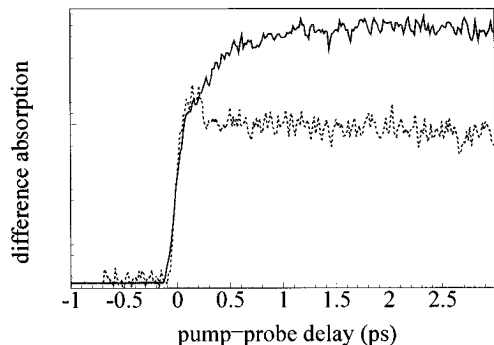


**Figure 3.** Comparison of the instantaneous and the 400 fs components of the pump-probe signals probed at 620 nm for  $I_2$  in pure mesitylene solution (solid line) and in a mesitylene/cyclohexane mixture (dotted line). The difference is due to secondary I:mes product formation in case of the pure solvent. The signal near zero delay in the mesitylene/cyclohexane mixture is due to free iodine.

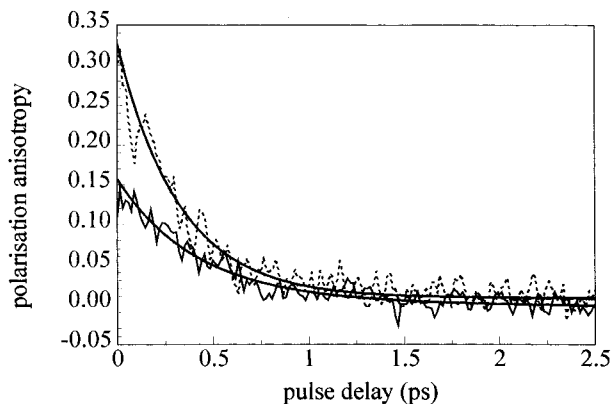


**Figure 4.** Plot of the polarization anisotropy at 620 nm after excitation at 310 nm of the  $I_2$ :mes complex in pure mesitylene solution (solid curve) and in a mesitylene/cyclohexane mixture (dotted curve). The heavy solid lines represent a (bi)exponential fit with time constants given in the text.

Fluctuations in the solvent heat bath can, of course, assist the barrier-crossing process or enhance curve crossing to a reactive potential.

Noteworthy is the fact that Figure 1 shows no indication of fast geminate recombination. As electron donors are known to catalyze the recombination process of free I atoms,<sup>31</sup> a rather strong cage effect was expected. Its absence here is surprising, especially in light of the results of Schwartz *et al.*,<sup>3</sup> who found that fast single-collision geminate recombination is very common in bond-breaking reactions. The lack of a cage effect in this reaction should bear directly on the mechanism of the dissociation process. This will be discussed further when the results of simulations are compared to the measurements.

A remarkable observation concerns the polarization anisotropy  $\rho$  of the I:mes photoproduct signal. Figure 4 displays the measured anisotropies both in pure arene and in mixed mesitylene/cyclohexane solutions. The polarization anisotropy is defined by<sup>32</sup>

$$\rho = \frac{S_{\parallel} - S_{\perp}}{S_{\parallel} + 2S_{\perp}} \quad (2)$$

where  $S_{\parallel}$  ( $S_{\perp}$ ) represents the intensity of the pump-probe signal obtained with parallel (perpendicular) polarizations of pump and probe beams. It is a measure for the alignment of excited and probed transition dipole moments.<sup>32,33</sup> Thus, a rapid loss of polarization anisotropy means that a fast change occurs in the angle between the transition dipole in the I:mes complex and

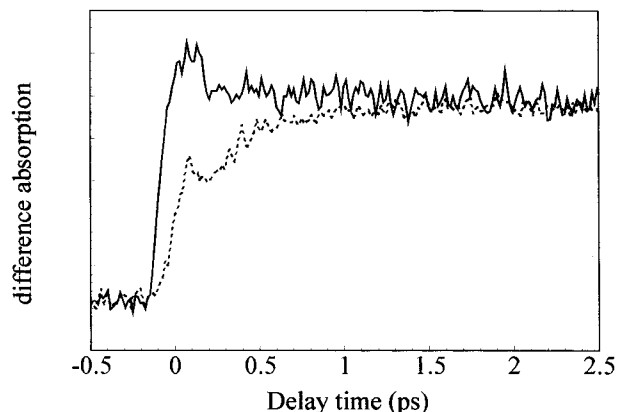


**Figure 5.** Pump-probe spectra on the  $I_2$ :mes complex in a mixed mesitylene/cyclohexane solution. The solid curve presents the signal when pump and probe are parallel polarized. The dotted curve was obtained for orthogonal polarization of the pump and probe. The pump wavelength was 310 nm, and the probe wavelength was set at 620 nm.

that of the parent  $I_2$ :mes complex. The heavy solid lines in Figure 4 represent a biexponential fit for pure mesitylene with time constants  $\tau_1 = 365 \pm 35$  fs (80%) and  $\tau_2 = 1.1 \pm 0.7$  ps (20%) and a single-exponential fit for a mixed mesitylene/cyclohexane solution with time constant  $\tau = 325 \pm 65$  fs.

The ps decay component observed for pure mesitylene solutions is assigned to rotational diffusion of the I:mes complex, although it is a little fast.<sup>25,34–36</sup> The 365 fs time scale, however, is about an order of magnitude too short to be attributed to this process. We conjectured in an earlier Letter<sup>24</sup> that this fast decay is caused by a forced rotation of the iodine atom:arene complex induced by the photodissociation process. An alternative option for the fast decay is secondary iodine atom:arene complex formation, which proceeds on the same time scale and whose polarization characteristics will be random. This effect would certainly lead to a fast decay of the polarization anisotropy. This option, however, seems to be less likely by the observation that the polarization anisotropy exhibits ultrafast decay for the mixed solution as well, where secondary complex formation is of lesser importance.

As photodissociation-induced rotation of the I:mes photofragment is one of the key issues in this paper, it seems worthwhile to discuss an experiment that strongly supports this concept. For this purpose consider the parallel ( $\parallel$ ) and perpendicular ( $\perp$ ) pump-probe (pu-pr) signals displayed in Figure 5. These signals pertain to the  $I_2$ :mes complex in mixed mesitylene/cyclohexane solution. Note that the signal near zero delay (overshoot) is due to free iodine. While the  $\parallel$  pu-pr signal in Figure 5 is basically constant, the  $\perp$  pu-pr signal grows in with a risetime of about 270 fs. These observations can only be reconciled by assuming that two dynamical processes occur at about the same time scale: a fast rotation of the I:mes photoproduct and a fast generation of secondary I:mes complexes. For parallel polarization these two processes have an opposite effect on the pu-pr signal: while rotation of the primary I:mes complex degrades the signal, formation of secondary I:mes complexes leads to a rise of it. In this mixed mesitylene/cyclohexane solution, these effects compensate one another. For  $\perp$  polarization the situation is completely different: here rotation of primary I:mes complexes and formation of secondary I:mes complexes both lead to an increase of the pu-pr signal. Figure 5 shows that after about 2–3 ps the  $\parallel$  and  $\perp$  pu-pr signals merge. The inescapable conclusion of these experiments must be that the primary I:mes complex undergoes a fast rotational process immediately after its formation.

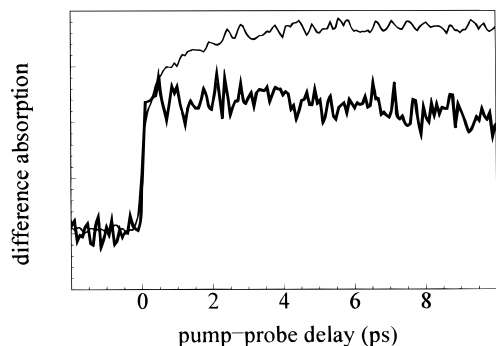


**Figure 6.** Pump-probe transients for  $I_2$  in pure toluene (light line) and toluene/cyclohexane mixture (heavy line), obtained by probing at 500 nm. The secondary product formation in pure toluene occurs on a picosecond time scale, which is much slower than in case of mesitylene (Figure 1).

We originally suggested<sup>24</sup> that this forced rotation of the complex resulted from the fact that the I-I-mesitylene bending motion was involved in the reaction coordinate, as was observed in the photodissociation of iodine cyanide<sup>37</sup> and dimethylnitrosamine.<sup>26,38</sup> The activation of this bending motion was also used to explain the low initial value of  $\rho$ : 0.1. We now believe that both effects are due to photoselection of bent  $I_2$ :ar complexes. This will be further discussed in section 4.

In accordance with earlier findings,<sup>22</sup> evidence was found for a second channel, next to the one leading to I-I dissociation.<sup>24</sup> Hilinski and Rentzepis<sup>22</sup> assigned the corresponding pump-probe transient to the positively charged mesitylene radical of the  $I_2$ :mes<sup>+</sup> charge-transfer complex, which they suggested to be the first product in the reaction. However, the transient spectrum of  $I_2^-$ , which is very well-known<sup>39,40</sup> and is centered at 720–740 nm, was not observed. Because of its spectral characteristics, we assigned the second channel to  $I_2$  that is expelled from the  $I_2$ :mes complex.<sup>24</sup> In view of the scarce information we have on this (dominant) reaction channel, we will not discuss it further here. However, future experiments are planned to further investigate this dissociation route in greater detail.

Figure 6 shows that for the system  $I_2$ :tol, similar transient absorptions were found, be it that the photoproduct now absorbs maximally at about 500 nm. This is in agreement with the reported spectrum of the I:tol complex.<sup>23</sup> Formation of secondary I:tol complexes is also observed, as Figure 6 shows, but at a slower pace, which is to be expected for a weaker electron donor such as toluene. Because of the poor quality of the continuum, it was not possible to measure the polarization anisotropy of this signal. The signatures of a second photochemical channel are also clearly observed as a 15 ps bleach recovery at 310 nm. These findings show that the photodynamics of  $I_2$ :mes and  $I_2$ :tol are very similar.

**3.2. Resonance Raman Experiments.** Resonance Raman spectroscopy has proven to be an excellent tool for investigation of ultrafast excited-state dynamics. Especially, the work by Heller and co-workers<sup>41,42</sup> led to a profound grasp of the relation between resonant Raman intensity and wave packet propagation. Kinsey and co-workers applied these ideas more quantitatively to a number of gas phase photodissociation reactions,<sup>43–45</sup> thus providing some beautiful pictures about the dynamics along the reaction path. Subsequent studies by Mathies and Myers<sup>46</sup> demonstrated that the technique could also be applied to liquid phase dynamics, provided that the system studied has a low fluorescence quantum yield.

The resonance Raman spectra of  $I_2$  in pure mesitylene have been recorded for excitation wavelengths ranging from 290 to

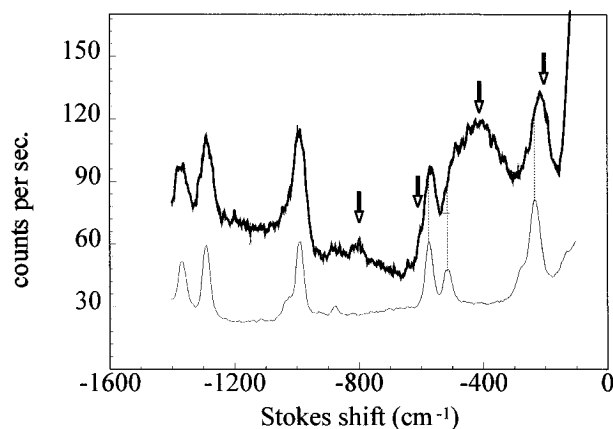


**Figure 7.** Raman spectrum of  $I_2$  in mesitylene, obtained by exciting at 349 nm. The Raman spectrum of pure mesitylene is given by the light line. Arrows indicate the  $I_2$  Raman lines at the fundamental vibration frequency at 200  $cm^{-1}$  and the first three overtones.

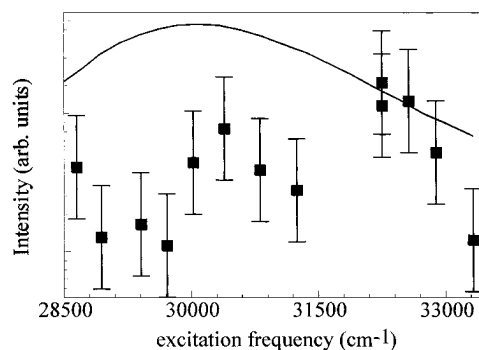
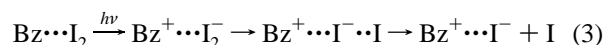


**Figure 8.** Excitation profile of the  $\nu = 4 \leftarrow \nu = 0$  Raman transition ( $800\text{ cm}^{-1}$ ) of the I-I stretching vibration of  $I_2$  in mesitylene. The solid line presents the room temperature absorption spectrum of the  $I_2$ :mes complex in mesitylene.

350 nm, which cover the largest part of the  $I_2$ :mes CT absorption band. Although not very pronounced, the stretch vibration of  $I_2$  was observed up to its third overtone; Figure 7 displays a typical spectrum. For comparison the Raman spectrum of pure mesitylene is also presented. Noteworthy is the fact that the first overtone falls into a spectral region that shows strong resonance enhancement from other CT complex vibrations as well. We may witness here resonance enhancement of the I-I-mesitylene bending type motions. Since we have no further information on these motions, we have not investigated this spectral region in detail. The  $I_2$  vibrational progression is comparable to the case of resonance enhancement by the B absorption band of  $I_2$  in the visible region.<sup>47</sup>

Figure 8 shows the excitation profile of the third overtone, which is the  $I_2$  Raman peak most clearly separated from mesitylene peaks. The CT transition of  $I_2$ :mes in this spectral region is also displayed. Obviously, the intensity of the  $I_2$ -stretch vibration does not track the absorption spectrum of the CT transition, although it is somewhat enhanced.

For a fast ( $< 25$  fs) reaction along the I-I internuclear coordinate, substantial resonance enhancement is expected,<sup>41,42</sup> unless the system undergoes curve crossing to a potential surface that exhibits a small transition dipole with respect to the ground state. A possible candidate for such a surface is an intermediate state in the "harpoon" reaction path, discussed by Cheng *et al.*<sup>28</sup> In the harpoon reaction mechanism the sequence of events is as follows:



If this picture of the reaction is correct, charge redistribution in the excited state is the rate-determining step in case of an isolated complex. In the liquid state bath fluctuations promote the complex to this transition state at a rate faster than the photodissociation process itself. The presence of a solvent bath thus provides a source of free energy that can drive the reaction across the barrier. The solvent also provides the possibility to function as a heat sink for the electronic degrees of freedom, allowing rapid curve crossing to take place.

The seemingly erratic shape of the excitation profile can be caused by an excitation energy dependence of the predissociation efficiency. The rapid curve crossing then leads to a reduction of resonance enhancement. It is suggestive that the “dips” in the excitation profile, at around 29 000 and 31 500  $\text{cm}^{-1}$ , are located around the vertical transition energies to two known excited states of  $\text{I}_2$ .<sup>48</sup>

**4. Charge-Transfer Excitation.** In a charge-transfer state, a net amount of electron density is transferred from a donor to an acceptor molecule. Mulliken<sup>10</sup> was the first to provide a theoretical description of this effect in terms of a two-level system consisting of a ground state  $\Psi_g$  and an excited state  $\Psi_e$ :

$$\begin{aligned}\Psi_g &= a\Psi(\text{D},\text{A}) + b\Psi(\text{D}^+, \text{A}^-) \\ \Psi_e &= a'\Psi(\text{D}^+, \text{A}^-) - b'\Psi(\text{D},\text{A})\end{aligned}\quad (4)$$

Here  $a \approx a'$ ,  $b \approx b'$ ,  $a \gg b$ ,  $\Psi(\text{D},\text{A})$  is constructed from donor and acceptor orbitals, and  $\Psi(\text{D}^+, \text{A}^-)$  is the state where an electron is transferred. The magnitude of the transition dipole for the excitation from  $\Psi_g$  to  $\Psi_e$  depends on the constant  $b$ , which is determined by the properties of donor and acceptor orbitals and their overlap. In the following we will take benzene as a model for mesitylene and toluene. In view of the small differences found for  $\text{I}_2$ :mes and  $\text{I}_2$ :tol, we assume the  $\text{I}_2$ :ben complex to exhibit the same dynamics.

The highest occupied molecular orbital (MO) in benzene is a doubly degenerate  $e_{1g}$  state in the  $\pi$  system, while the lowest unoccupied MO in  $\text{I}_2$  is the  $5p\sigma^*$  orbital. For  $\text{I}_2$  in the axial position, the point group of the complex is  $C_{6v}$ . As pointed out by Walker *et al.*,<sup>27</sup> this leads to a degenerate transition dipole which lies in the  $xy$ -plane of the benzene ring. Distortion of the complex from axial symmetry removes the degeneracy of the excited CT state and leads to a single direction for the in-plane component of the transition moment. It also generates a transition moment along the out-of-plane axis, perpendicular to the ring. For  $\text{I}_2$  in the resting position, the point group of the complex is  $C_{2v}$ , and the excited CT states are split into two states with  $A_1$  and  $A_2$  symmetry. The transition to  $A_1$  (along the  $z$ -axis) is allowed, while the transition to  $A_2$  is forbidden.

In liquids, many conformations of the  $\text{I}_2$ :ar complex are present (*vide infra*). In order to determine how the transition dipole moment depends on the various conformations of the  $\text{I}_2$ :ben complex, a semiempirical configuration-interaction calculation was performed.

The calculations were performed with the ZINDO program<sup>49</sup> on a Macintosh II CE CaChe workstation. For every investigated conformation, the lowest 10 excited states were computed. Two CT transitions (benzene  $e_{1g}$  to  $\text{I}_2$   $\sigma^*$ ) were obtained. The strongest one was located in the spectral region of 280–300 nm, depending on the conformation of the oblique  $\text{I}_2$ :ben complex. The perturbed visible–iodine transition in the complex was found around 450 nm. Both predictions are in fair agreement with experiment. Also, the calculated relative oscillator strengths ( $\sim 8$ ) of the CT versus the perturbed iodine transition (averaged over all orientations of the iodine molecule

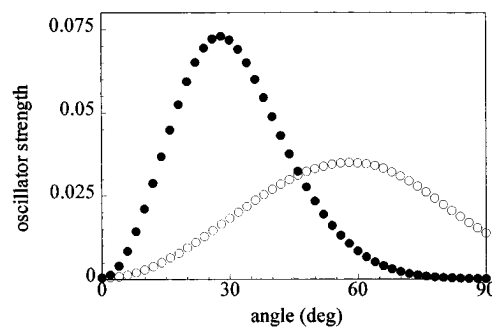


**Figure 9.** Oscillator strength of the CT transition of  $\text{I}_2$ :ben as a function of the angle between the 6-fold axis of the benzene ring and the molecular axis of the  $\text{I}_2$  molecule. The filled symbols represent the conformations where the  $\text{I}_2$  molecule was pivoted around its center of mass, and the open symbols represent the conformations where the  $\text{I}_2$  molecule was pivoted around the I atom nearest to the benzene ring. The axial conformation corresponds to an angle of  $0^\circ$  and the resting conformation to  $90^\circ$ .

in an oblique configuration) agree well with experiment. However, while the relative oscillator strengths are calculated correctly, the absolute values are off by a factor of 10. This is a recognized weakness of ZINDO which is caused by the fact that only a limited basis set is used in the configuration-interaction calculations. For all oblique conformations of the  $\text{I}_2$ :ben complex, the in-plane transition moment was found to be roughly 10 times smaller than the out-of-plane one. The only exception is the exact axial conformation, where the out-of-plane transition moment vanishes by symmetry. The splitting between the  $A'$  and  $A''$  states in the oblique conformation is at most  $800 \text{ cm}^{-1}$ , depending on the orientation of the iodine molecule.

The CT wave functions and state energies of the  $\text{I}_2$ :ar complex were calculated as a function of angle between the benzene symmetry axis and the  $\text{I}_2$  molecular axis for two types of conformations. In the first series, the  $\text{I}_2$  molecule was pivoted around its center of mass. In the second series, it was rotated around the I atom nearest to the benzene ring. In both cases a plane of symmetry was preserved. Figure 9 depicts the oscillator strength of the strongest CT transition as a function of rotation angle for both sets of conformations. With the exception of the axial conformation, the direction of the transition dipole moment was found to be pointing (within  $\sim 10^\circ$ ) from the center of the benzene ring to the  $\text{I}_2$  center of mass for all investigated conformations. At zero angle, the oscillator strength is very small ( $\sim 0.0004$ ). Upon increasing the angle by pivoting around the  $\text{I}_2$  center of mass (oblique conformation), the oscillator strength increases rapidly, reaching a maximum of 0.073 at an angle of ca.  $30^\circ$ . For larger angles the oscillator strength decreases, mainly because of the increased distance between the  $\text{I}_2$  centroid  $\sigma^*$  MO and the overlap region with one of the benzene  $e_{1g}$  orbitals. When the  $\text{I}_2$  molecule is rotated around the I atom nearest to the benzene ring, the oscillator strength increases more slowly, reaching a broad maximum of 0.035 at an angle of  $\sim 60^\circ$ .

When the iodine molecule is rotated over  $90^\circ$  around its center of mass, the distance from the benzene ring to  $\text{I}_2$  is larger than in the equilibrium conformation of the resting structure. To ascertain that this does not lead to an unrealistically low value for the oscillator strength at near-resting conformations, a number of resting conformations with varying  $\text{I}_2$ –benzene distance were evaluated. It turns out that even at the equilibrium distance, the oscillator strength of the CT transition is only 0.001.

The conclusion of these calculations therefore is that the oscillator strength of the  $\text{I}_2$ :ar charge-transfer transition depends

greatly on the conformation of the complex. The largest oscillator strength is obtained for the oblique conformation where the I<sub>2</sub> molecule is pivoted around its center of mass, making an angle of ~30° compared to the axial structure. This result accords with the fact that the more stable complexes in the I<sub>2</sub>:ar series, for which the deviation from the fully axial position is smallest, have the lowest oscillator strengths.<sup>9,50</sup> If a wide distribution of conformations exists, photoselection will occur in pump–probe experiments of complexes with the largest transition moment. In other words, the excitation process selects I<sub>2</sub>:ar complexes that are bent!

Besides the transition dipole, the energy of the CT state depends also on the conformation of the I<sub>2</sub>:ar complex. This suggests that part of the spectral width of the CT transition is inhomogeneous in nature and that by changing the excitation wavelength one selects certain configurations of the CT complex. Whether photoselection occurs, depends, of course, on the homogeneous solvent dynamics as well.

## 5. Molecular Dynamics Simulations

To examine the structure and stability of the I<sub>2</sub>:ar CT complexes and simulate the photochemical process, a molecular dynamics (MD) study was performed. In this section, a brief summary will be given of the methods and some of the results. Details of the calculations will be published elsewhere.<sup>51</sup> Again benzene was chosen as a model system for mesitylene and toluene, because of computational reasons and the fact that a number of MD simulations exist for pure benzene.<sup>18,52,53</sup>

The computational study was set up as follows. *Ab initio* calculations on the I<sub>2</sub>:ben and I:ben complexes were performed using the GAMESS (generalized atomic and molecular electronic structure system) suite of programs,<sup>54</sup> in order to obtain the necessary force field parameters for the MD simulations. Both complexes were treated as supermolecules. The core electrons were taken into account by the effective core potentials of Hay and Wadt.<sup>55</sup> For the I<sub>2</sub>:ben complex, the restricted Hartree–Fock self-consistent field (HF-SCF) method was used, while for the I:ben complex the unrestricted HF-SCF method was employed. For both complexes, Møller–Plesset second-order energy corrections were included. Because of the size of the system, configuration-interaction calculations were not feasible. The calculations were performed for various conformations of the complexes, as a function of the I–ben or I<sub>2</sub>–ben distance. The results were fit to a site–site isotropic Buckingham–Coulomb potential force field, one for either complex.

The MD calculations were performed using the GROMACS (Groningen machine for chemistry simulation) package.<sup>56</sup> Two types of MD runs were performed, which can be classified as equilibrium runs and photodissociation runs. The equilibrium runs made use of the force field parameters of the I<sub>2</sub>:ben complex. For the photodissociation runs, snapshots from the equilibrium runs were taken as starting situations. At the time of I–I bond rupture, the binding potential from the equilibrium runs was replaced by a repulsive one. At the same time the force field was switched to that of I:ben.

From the *ab initio* calculations, the I<sub>2</sub>:ben complex is found to be weakly bound in the axial conformation and hardly bound at all in the resting conformation. The binding energy found for the axial structure is 737 cm<sup>-1</sup>, which is in good agreement with the experimental value<sup>17</sup> of 770 cm<sup>-1</sup>, as well as with the one calculated by Kochanski and Prissette.<sup>15</sup>

The equilibrium MD simulations were used to evaluate the stability of the complexes. The time that an I<sub>2</sub> molecule spends near a particular benzene molecule before moving on to the

next one was, on average, found to be about 0.2 ps. This is a factor of 3–4 shorter than the one deduced from a Raman study by *Besnard et al.*<sup>13</sup> However, in view of the simplistic model used in the analysis of the Raman data, the agreement is considered satisfactory. A discrepancy between theory and experiment may also be caused by the inability of the MD program used to describe varying polarization of the I<sub>2</sub> molecule. Part of the binding energy of the I<sub>2</sub>:ben complex is caused by the slight polarization of I<sub>2</sub> by benzene.<sup>57,58</sup> This effect also follows from the *ab initio* results and is incorporated in the MD force field. However, because of the shifted charge, a benzene molecule approaching an I<sub>2</sub> molecule from the other side will be slightly repelled by it. In the MD calculations, this effect is absent and the I<sub>2</sub> molecule is free to move from one benzene molecule to the next.

As input for the photodissociation MD simulations, we need to assess how much energy may be deposited in the fragments after photodissociation. This, of course, depends crucially on the initial and final states involved in the dissociation process. After bond breaking, the energy available for translational motion of the fragments,  $E_{\text{tr}}$ , varies from 1 to 3 eV, depending on the exit channel.<sup>48</sup> Because of the ultrafast dissociation process we assumed the reaction to proceed on a one-dimensional repulsive surface. For this potential an exponential shape was assumed, with a slope of  $-E_{\text{tr}} \text{ cm}^{-1} \text{ \AA}^{-1}$  at the ground-state equilibrium bond length of 2.67 Å.

To investigate the dynamics of the polarization anisotropy in the I:ben CT transition, the time evolution of the transition dipole vector was extracted from the photodissociation runs. Secondary iodine atom:ben complex formation was also taken into account by selecting the benzene molecule closest to the ejected iodine atom as partner for complex formation. The built-up time in this channel was taken to be 400 fs, in accordance with the observed secondary complex formation, discussed in section 3.1 (Figure 1). The transition dipole in the CT complex was taken to point from the I<sub>2</sub> center to the benzene center of mass. For the I:ben complex, the transition dipole was assumed to point along the vector connecting the I atom and the benzene center of mass. This latter assumption is the more questionable one. First of all, the iodine atom will be slightly displaced after the iodine–iodine bond is broken. Second, the transition dipole may not necessarily point along the I:ben center-of-mass direction. We stress, however, that the transition dipole for I:ben is not in the benzene plane, for similar reasons as discussed for the I<sub>2</sub>:ben case. We thus propose that the probing process is also selective.

The important point to realize is that while the initial value of polarization anisotropy is sensitive to these assumptions the decay of the anisotropy is much less so. The polarization anisotropy<sup>32,33</sup> can be calculated from the angle  $\theta$  between excited and probed transition dipoles through the following well-known relation:<sup>24</sup>

$$\rho(t) = (3/5)\langle \cos^2 \theta(t) \rangle - 1/5 \quad (5)$$

where  $t$  denotes the time elapsed since the beginning of the dissociation and the brackets denote averaging over all photodissociation runs.

The calculations were performed on oblique I<sub>2</sub>:ben complexes with configurations around those that exhibited the largest CT oscillator strength according to our calculations. These MD runs will be termed “biased” in the remainder of this paper. In order to mimic this situation, a set of artificial weak bonds was added between an I<sub>2</sub> molecule and a particular benzene molecule in the equilibrium runs, to restrict axial motion of the I<sub>2</sub> molecule within a window of roughly 30 ± 15°. It must be

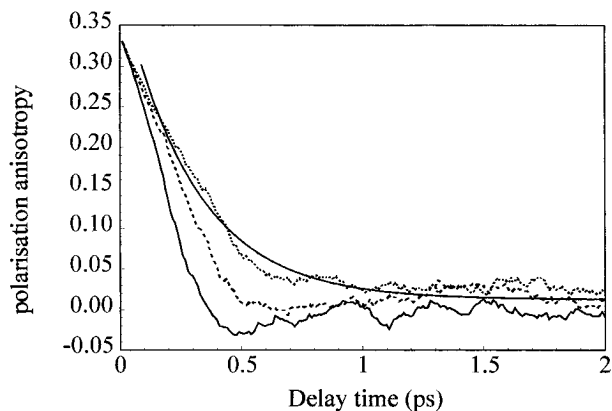


**Figure 10.** Polarization anisotropy  $\rho(t)$  for the I:ben photoproduct calculated from molecular dynamics simulations for different energy disposals in the fragments. Each curve is based on 100 runs. From bottom to top the energy disposal is 20 000 (solid line), 10 000 (dashed line), and 5000  $\text{cm}^{-1}$  (dotted line). The light line through the upper curve presents a single-exponential fit with a time constant of 300 fs. The calculations were done for selected (biased) oblique conformations of the complex (see text).

emphasized that no physical significance may be attributed to the artificial bonds; they were included only because it is computationally easier to constrain the conformation in the calculations than to select the proper conformations afterward.

The polarization anisotropies  $\rho(t)$  as calculated from the MD simulations for different energies in the fragments are displayed in Figure 10. This figure shows, not unexpectedly, that the decay of  $\rho(t)$  strongly depends on the energy deposited into the fragments. The more energy that is available for translational motion of the fragments, the faster the decay of the polarization anisotropy. For energy disposals of 20 000 and 10 000  $\text{cm}^{-1}$ , single-exponential fits to the calculated anisotropies yield decay times of 102 and 164 fs, respectively. When 5000  $\text{cm}^{-1}$  is put into fragment motion, the polarization anisotropy decays in about 300 fs, which is close to the experimental time scale. The calculated initial anisotropy ( $\sim 0.35$ ) agrees fairly well with the experimental value for a mesitylene/cyclohexane solution, but not with that of pure mesitylene (Figure 4). This will be discussed below.

No evidence of caging of the I atoms was observed. After the excess kinetic energy of the I atoms is transferred to benzene, which takes roughly 3 ps, the interatomic distance stabilizes between 7 and 14 Å, which is too large for cage recombination.

## 6. Discussion

The most direct way to compare simulations and experiments is through the polarization anisotropy. The decay of the calculated anisotropy  $\rho(t)$  agrees well with the experimental time scale when about 5000  $\text{cm}^{-1}$  is deposited as kinetic energy in the fragments. One should note that the MD calculations were done for benzene and not for mesitylene for which we have the experimental data. If the calculations had been done for mesitylene, one would expect that more energy disposal in the fragments would be needed to obtain the same decay time of the polarization anisotropy than for benzene, because of the larger mass of mesitylene. This implies that the 5000  $\text{cm}^{-1}$  should be considered a lower limit for mesitylene. For the physics behind the fast decay of the polarization anisotropy, the following picture emerges. Upon photodissociation of the I<sub>2</sub>:ben complex, the I atom nearest to the benzene moves toward the latter, pushes it away, and thereby forces it to rotate, although it is hindered by the other benzene molecules. This forced rotation causes the rapid decay of the polarization anisotropy.

In this picture, it is not necessary to invoke a bent transition state;<sup>24</sup> rather, one can see it as a “cat flap” mechanism on a molecular scale. As the calculated time scale corresponds well to the experimental one, it is warranted to conclude that photoselection of bent molecules is the crucial factor to explain the rapid decay of the polarization anisotropy.

The MD simulations overestimate the initial anisotropy (Figure 4). This discrepancy could be due to the fact that the notion of an isolated I<sub>2</sub>:ben complex in pure benzene is oversimplified. It is not unlikely that the iodine molecule in the I<sub>2</sub>:ben complex interacts in a significant way also with other nearby benzene molecules. This effect would counteract the predicted dependence of the oscillator strength on the conformation of the CT complex and thus act against photoselection as well. Preliminary MD simulations in which all I<sub>2</sub>:ben configurations are given equal weight indeed yield a lower initial anisotropy.

The observed initial anisotropy of  $0.34 \pm 0.06$  of I:mes in cyclohexane agrees well with the idea that the transition dipoles in I<sub>2</sub>:mes and I:mes are parallel. The fact that anisotropy decays on the same fast time scale as in pure mesitylene confirms the idea that this decay is due to forced rotation of the I:mes complex and not to secondary I:mes complex formation. Although the secondary complexes have a distinct contribution to the polarization anisotropy, their effect on the overall signal is limited. This is caused by the finite built-up time of these complexes, which is of the same order of or slower than the decay of the anisotropy itself. These results will be discussed in a future paper on MD simulations of the I<sub>2</sub>:ben complex.<sup>51</sup>

The rotational energy that is initially deposited in the I:mes photoproduct can be estimated by using a model that was developed to describe the reversible dephasing of a rotational wave packet in a gas phase molecule.<sup>59</sup> From this model, it follows that the average rotational energy is

$$\langle E_r \rangle \approx \frac{4.8}{(B/\text{cm}^{-1})(\tau/\text{ps})^2} \text{cm}^{-1} \quad (6)$$

where  $B$  is the rotational constant of the fragment and  $\tau$  is the dephasing time of the rotational wave packet. By equating  $\tau$  with the observed depolarization time constant of 365 fs and by estimating  $B = 0.02 \text{ cm}^{-1}$  for the rotational constant of the I:mes fragment, we calculate  $\langle E_r \rangle \sim 2000 \text{ cm}^{-1}$ . This is about 80% of the kinetic energy that one photofragment has available after the dissociation. According to the MD calculations, the I atom uses the remaining kinetic energy to move out of the solvent cage; this is transferred to the environment on a 3 ps time scale. Note that the application of eq 6 is warranted only when the rotational motion of the photoproduct is inertial. Optical Kerr-effect measurements show that this assumption is valid for the first few hundred femtoseconds in benzene liquid.<sup>35,60</sup>

The model presented for the photodissociation reaction accounts also for the absence of fast geminate recombination of the I:ar and I atom fragments. Due to the forced rotation of the I:ar fragment, the products are not able, before escaping from the solvent cage, to regain the proper position for a reunion. This is confirmed by the simulation; the I atoms leave the solvent cage on the same time scale as that on which the rotation takes place, in a few hundred femtoseconds, and do not return.

In the unbiased photodissociation runs,<sup>51</sup> escape from the solvent cage also occurs. If the I atom does not collide head-on with a benzene ring, there is enough space for the I atom to move relatively unhindered between the benzene molecules. This can be understood from the structure of the benzene liquid, in which quadrupole–quadrupole interactions dominate.<sup>61</sup> This



stabilizes the T-stack arrangement of the benzene molecules, which leaves large holes in the structure of the liquid.

## 7. Conclusions

From femtosecond transient absorption studies on I<sub>2</sub>:ar CT complexes in different solvents, it is confirmed that photodissociation of molecular iodine in these weakly bound CT complexes occurs within 25 fs. The photoselected complexes have a bent structure with the iodine molecule rotated by 30° from the axial position. Since resonance Raman spectra—while exciting into the charge-transfer band—exhibit little resonance enhancement for the I<sub>2</sub> vibration, rapid curve crossing is assumed to occur from the initially excited charge-transfer state to a lower state, from which dissociation takes place. The suggested harpoon mechanism for this reaction would allow for such an intermediate “dark” state. The observed rapid decay of the polarization anisotropy in the absorption transient of the I:ar product is ascribed to forced rotation of the I:ar product induced by energy disposal in the fragments following the photodissociation process. Molecular dynamics simulations confirm the earlier suggested fragility of the I<sub>2</sub>:ar complex and yield a proper time scale for the decay and initial value of the polarization anisotropy, provided about 5000 cm<sup>-1</sup> is released into the fragments. Future research on this system will center on the concurrent reaction path in which molecular iodine is ejected; especially, the question whether or not I<sub>2</sub> is vibrationally excited will be investigated. Full understanding of the photophysics of this prototype charge-transfer system remains the ultimate goal of our efforts. The present work shows that MD simulations can play an important role in the interpretation of ultrafast spectroscopic experiments as well as stimulate thinking about new experiments.

## Note Added

Shortly after this paper had been submitted, two papers came out on the iodine–arene charge-transfer complex. Pullen *et al.*<sup>62</sup> reported on femtosecond pump–probe studies of the iodine:mes complex. Many of their findings accord with ours,<sup>24</sup> but there are also some significant differences. For instance, they find much longer decay times of the polarization anisotropy than those reported by us, a different branching ratio for iodine bond breaking versus iodine expulsion from the I<sub>2</sub>:mes complex, and substantial geminate recombination of I atoms with the I:mes complex. These facts accord with the notion that with excitation at 400 nm (Pullen *et al.*), about 7000 cm<sup>-1</sup> less energy is available for deposition in the fragments than for excitation at 310 nm. Pullen *et al.*<sup>62</sup> point out also that secondary I:mes complex formation might be responsible for the ultrafast decay of the polarization anisotropy reported in ref 24. In this paper we have shown that this effect, although certainly present, has little impact on the decay of the polarization anisotropy. Cheng *et al.*<sup>63</sup> recently reported an update on their photodissociation studies of the I<sub>2</sub>:ben complex in the gas phase, detecting the ejected iodine atoms by mass spectrometric techniques. They show that the low translational energy disposal in the iodine atoms is consistent with a harpoon mechanism for dissociation of the I<sub>2</sub>:ben complex. The very different reaction rate observed in the gas phase for I<sub>2</sub>:mes (~1 ps) compared to that in solution (~25 fs) suggests that barrier crossing to the exit channel(s) is stimulated by the presence of a heat bath. It is also possible that solvation has lowered a barrier to a reaction path in solution that is not accessible in the gas phase.

**Acknowledgment.** The investigations were supported by the Netherlands Foundations for Physical Research (FOM) and

Chemical Research (SON) with financial aid from the Netherlands Organisation for the Advancement of Science (NWO). The resonance Raman experiments, performed at LENS, were supported by the Commission of the European Communities under Contract No. GE1\*CT92-0046. E.L. thanks Professor R. Righini and Professor S. Califano of LENS for their hospitality and for their help in organizing his visit to Florence. D.A.W. and F.E. would like to thank Prof. Herman J. C. Berendsen for the hospitality and help provided by the Groningen-MD group. We gratefully acknowledge discussions with Dr. Piet T. van Duijnen on the semiempirical calculations of the I<sub>2</sub>:ben complex and his help in getting us acquainted with ZINDO. We are also grateful to one of the referees for critical perusal of the manuscript.

## References and Notes

- (1) *Femtosecond Reaction Dynamics*; Wiersma, D. A., Ed.; North-Holland: Amsterdam, 1994. *Femtosecond Chemistry*; Manz, J., Wöste, L., Eds.; VCH: New York, 1994.
- (2) Smith, D. E.; Harris, C. B. *J. Chem. Phys.* **1987**, *87*, 2709.
- (3) Schwartz, B. J.; King, J. C.; Zhang, J. Z.; Harris, C. B. *Chem. Phys. Lett.* **1993**, *203*, 503.
- (4) Yan, Y. J.; Whitnell, R. M.; Wilson, K. R.; Zewail, A. H. *Chem. Phys. Lett.* **1992**, *193*, 402. Li, Z.; Zadayan, R.; Apkarian, V. A.; Martens, C. C. *J. Phys. Chem.* **1995**, *99*, 7453.
- (5) Martin, J. L.; Breton, J.; Hoff, A. J.; Migus, A.; Antonneti, A. *Proc. Natl. Acad. Sci. U.S.A.* **1986**, *83*, 957.
- (6) Park, H. W.; Kim, S. T.; Sancar, A.; Deisenhofer, J. *Science* **1995**, *268*, 1866.
- (7) Hagfeldt, A.; Gratzel, M. *Chem. Rev.* **1995**, *95*, 49.
- (8) Johnson, A. E.; Levinger, N. E.; Walker, G. C.; Barbara, P. F. In *Ultrafast Phenomena VIII*; Martin, J. L., Migus, A., Eds.; Springer-Verlag: Berlin, New York, 1992; p 576.
- (9) Benesi, H. A.; Hildebrand, J. H. *J. Am. Chem. Soc.* **1949**, *71*, 2703.
- (10) Mulliken, R. S. *J. Am. Chem. Soc.* **1950**, *72*, 600.
- (11) Mulliken, R. S. *J. Am. Chem. Soc.* **1952**, *74*, 811.
- (12) Kiefer, W.; Bernstein, H. J. *J. Raman Spectrosc.* **1973**, *1*, 417.
- (13) Besnard, M.; del Campo, N.; Cavagnat, R. M.; Lascombe, J. *Chem. Phys. Lett.* **1989**, *162*, 132.
- (14) Fredin, L.; Nelander, B. *J. Am. Chem. Soc.* **1974**, *96*, 1672.
- (15) Kochanski, E.; Prissette, J. *Nouv. J. Chim.* **1980**, *4*, 509.
- (16) Jano, I. *Theor. Chim. Acta* **1985**, *66*, 341.
- (17) McLean, T. D.; Ratcliff, B. B.; Pastalan, J. Z.; Innes, K. K. *J. Quant. Spectrosc. Radiat. Transfer* **1989**, *42*, 445.
- (18) Danten, Y.; Guillot, B.; Guissani, Y. *J. Chem. Phys.* **1992**, *96*, 3782.
- (19) Logan, S. R.; Bonneau, R.; Jousot-Dubien, J.; Fournier de Violet, P. *J. Chem. Soc., Faraday Trans. 1* **1975**, *71*, 2148.
- (20) Rand, S. J.; Strong, R. L. *J. Am. Chem. Soc.* **1960**, *82*, 5.
- (21) Langhoff, C. A.; Gnädig, K.; Eisenthal, K. B. *Chem. Phys.* **1980**, *46*, 117.
- (22) Hilinski, E. F.; Rentzepis, P. M. *J. Am. Chem. Soc.* **1985**, *107*, 5907.
- (23) Strong, R. L.; Rand, S. J.; Britt, J. A. *J. Am. Chem. Soc.* **1960**, *82*, 5053.
- (24) Lenderink, E.; Duppen, K.; Wiersma, D. A. *Chem. Phys. Lett.* **1993**, *211*, 503.
- (25) McMorrow, D.; Lotshaw, W. T. *J. Phys. Chem.* **1991**, *95*, 10395.
- (26) Dubs, M.; Brühlmann, U.; Huber, J. R. *J. Chem. Phys.* **1986**, *84*, 3106.
- (27) Walker, L. A., II; Pullen, S.; Donovan, B.; Sension, R. J. *Chem. Phys. Lett.* **1995**, *242*, 177.
- (28) Cheng, P. Y.; Zhong, D.; Zewail, A. H. *Chem. Phys. Lett.* **1995**, *242*, 369.
- (29) Lenderink, E.; Duppen, K.; Wiersma, D. A. *Chem. Phys. Lett.* **1992**, *194*, 403.
- (30) Heikal, A. A.; Chong, S. H.; Baskin, J. S.; Zewail, A. H. *Chem. Phys. Lett.* **1995**, *242*, 380.
- (31) Porter, G.; Smith, J. A. *Proc. Roy. Soc., Ser. A* **1961**, *261*, 28.
- (32) Albrecht, A. C. In *Progress in Reaction Kinetics*; Porter, G., Ed.; Pergamon Press: Oxford, 1970; Vol. 5, p 301.
- (33) Feofilov, P. P. *The Physical Basis of Polarized Emission*; Consultants Bureau: New York, 1961; original version (in Russian); State Physico-Mathematical Press: Moscow, 1959.
- (34) Kalpouzou, C.; McMorrow, D.; Lotshaw, W. T.; Kenney-Wallace, G. A. *Chem. Phys. Lett.* **1988**, *150*, 138.
- (35) McMorrow, D.; Lotshaw, W. T. *Chem. Phys. Lett.* **1993**, *201*, 369.
- (36) Righini, R. *Science* **1993**, *262*, 1386.
- (37) Nadler, I.; Mahgerefteh, D.; Reisler, H.; Wittig, C. *J. Chem. Phys.* **1985**, *82*, 3885.

- (38) Lenderink, E.; Wiersma, D. A. *Chem. Phys. Lett.* **1994**, 218, 586.  
(39) Fournier de Violet, P.; Bonneau, R.; Jousot-Dubien, J. *Chem. Phys. Lett.* **1974**, 28, 569.  
(40) Banin, U.; Ruhman, S. *J. Chem. Phys.* **1993**, 98, 4391.  
(41) Lee, S. Y.; Heller, E. J. *J. Phys. Chem.* **1979**, 71, 4777.  
(42) Heller, E. J.; Sundberg, R. L.; Tannor, D. J. *J. Phys. Chem.* **1982**, 86, 1822.  
(43) Imre, D.; Kinsey, J.; Field, R.; Katayama, D. *J. Phys. Chem.* **1982**, 86, 2564.  
(44) Imre, D.; Kinsey, J. L.; Sinha, A.; Krenos, J. *J. Phys. Chem.* **1984**, 88, 3956.  
(45) Sundberg, R. L.; Imre, D.; Hale, M. O.; Kinsey, J. L.; Coalson, R. D. *J. Phys. Chem.* **1986**, 90, 5001.  
(46) Myers, A. B.; Mathies, R. A. *J. Chem. Phys.* **1984**, 81, 1552.  
(47) Xu, J.; Schwentner, N.; Chergui, M. *J. Chem. Phys.* **1994**, 101, 7381.  
(48) Mulliken, R. S. *J. Chem. Phys.* **1971**, 55, 288.  
(49) Edwards, W. D.; Zerner, M. C. *Theor. Chim. Acta* **1987**, 72, 347.  
(50) Murrell, J. N. *J. Am. Chem. Soc.* **1959**, 81, 5037.  
(51) Everdij, F. P. X.; Lenderink, E.; van der Spoel, D.; Mavri, J.; Wiersma, D. A. Manuscript in preparation.  
(52) Anderson, J.; Ullo, J. J.; Yip, S. *J. Chem. Phys.* **1987**, 86, 4078.  
(53) Yashonath, S.; Price, S. L.; McDonald, I. R. *Mol. Phys.* **1988**, 64, 361.  
(54) Schmidt, M. W.; Baldrige, K. K.; Boatz, J. A.; Elbert, S. T.; Gordon, M. S.; Jensen, J. J.; Koseki, S.; Matsunaga, N.; Nguyen, K. A.; Su, S.; Windus, T. L.; Dupuis, M.; Montgomery, J. A. *J. Comput. Chem.* **1993**, 14, 1347.  
(55) Hay, P. J.; Wadt, W. R. *J. Chem. Phys.* **1985**, 82, 270.  
(56) Berendsen, H. J. C.; van der Spoel, D.; van Drunen, R. *Comput. Phys. Commun.* **1995**, 91, 43.  
(57) Yarwood, J.; Person, W. B. *J. Am. Chem. Soc.* **1968**, 90, 594.  
(58) Lascombe, J.; Besnard, M. *Mol. Phys.* **1986**, 58, 573.  
(59) Zewail, A. H. *J. Chem. Soc., Faraday Trans. 2* **1989**, 85, 1221.  
(60) Waldman, A.; Banin, U.; Rabani, E.; Ruhman, S. *J. Phys. Chem.* **1992**, 96, 10842.  
(61) Hobza, P.; Selzle, H. L.; Schlag, E. W. *J. Chem. Phys.* **1990**, 93, 5893.  
(62) Pullen, S.; Walker, L. A., II; Sension, R. J. *J. Chem. Phys.* **1995**, 103, 7877.  
(63) Cheng, P. Y.; Zhong, D.; Zewail, A. H. *J. Chem. Phys.* **1995**, 103, 5153.

JP953325O